A Simple Test for the Suitability of Equilibrium Thickness

Jon E. Zufelt, PE, Ph.D.
Ice Engineering Research Division
U.S. Army Cold Regions Research and Engineering Laboratory
72 Lyme Road
Hanover, N.H. USA
jzufelt@crrel.usace.army.mil

Equilibrium ice thickness theory provides for a simple calculation of ice jam thickness given some basic information on river characteristics. There are several assumptions attendant with the use of equilibrium theory that may be violated by some numerical models. Highly unsteady flow situations demand the use of unsteady flow models in the determination of jam thickness. Gradually varying discharge situations, however, may find the use of equilibrium theory perfectly suitable, with minimal error in calculated jam thickness. A dimensionless parameter is proposed and demonstrated for use in determining whether simple equilibrium thickness calculations or a more complex unsteady model is required for the calculation of ice jam thickness.

1. Introduction

Ice jams form and evolve primarily through a variety of unsteady processes. A jam is formed when moving ice comes to rest, possibly with shoving and thickening because of the unsteady forces exerted by the water flow, jam weight, wind, ice strength, and frictional resistance. Once a jam forms, it may remain in an apparently stable condition for hours or days prior to failure. During this period of apparent stability, it is likely that many forces are actually changing. The jam's internal strength may be increasing via freeze-bonding of the individual ice pieces or it may be decreasing through thermal weakening of the ice mass. When a freezeup jam forms, the discharge is typically uniform and steady. The spring breakup period, however, is characterized by highly unsteady discharge resulting from rainfall on frozen ground, snowmelt, and surges caused by jam failure. Whether freezeup or breakup, however, jam formation results in increased water levels that may lead to flooding. The calculation of expected jam thickness and its effect on stage has been a topic of considerable interest since the late 1950's.

Early research efforts treated ice jams as stationary accumulations floating on a steady water flow. A major advance was the realization that a floating jam could be likened to a granular material contained between two parallel walls. The behavior of the jam is then influenced only by the forces exerted on it and its material properties. Zufelt and Ettema (1997) and Healy and Hicks (1997) provide excellent histories of the development of jam theory from the efforts of R.J. Kennedy (1958) through the present. Pariset and Hausser (1961) and then Pariset et al. (1966) formulated an equation to describe the balance of forces on a section of jam of "equilibrium thickness," with steady, uniform discharge in a uniform channel. For the typical case of a wide channel jam, the longitudinal force (F) grows with the distance downstream from the upstream edge of the jam, asymptotically approaching a maximum as the distance grows large. Their equation for the maximum longitudinal force acting through a wide jam is

$$F_{\max} = \frac{B}{2k_0\lambda}(\tau_i + f_3) - \frac{\tau_c \eta}{k_0 \lambda} \tag{1}$$

where B is the channel width, k_0 is the coefficient of lateral thrust (the ratio of lateral to longitudinal stress), λ is the friction coefficient of the ice on the bank, τ_i is the shear on the underside of the jam attributable to water flow, f_3 is the downstream component of the weight of the cover per unit area, τ_c is the cohesive stress per unit area at the banks, and η is the jam thickness.

Pariset et al. recognized that this maximum force, equal to the sum of the external forces, is resisted by the internal strength of the jam. If the external forces exceed the internal strength, the jam will fail and must thicken until there is once again a balance between the external forces and the jam strength. By treating the jam as a granular material, they likened the internal strength of the jam to that of a granular material under complete mobilization of the passive pressure resistance:

$$F_{\max} = K_p s_i \rho g (1 - s_i)\frac{\eta^2}{2} = \tan^2\left(\frac{\pi}{4} + \frac{\phi}{2}\right) s_i \rho g (1 - s_i)\frac{\eta^2}{2} \tag{2}$$

where K_p is the passive pressure coefficient (the ratio of longitudinal to vertical stress at failure), s_i is the specific gravity of ice, ρ is the density of water, g is the acceleration due to gravity, and ϕ is the angle of internal resistance of the accumulated broken ice, which is commonly taken as the angle of repose for granular materials. Combining equations 1 and 2 results in an expression relating jam thickness to the stresses exerted on it:

$$s_i \rho g (1 - s_i)\frac{\eta^2}{2} = \frac{B}{2\mu}(\tau_i + f_3) - \frac{\tau_c \eta}{\mu} \tag{3}$$

in which the coefficient μ represents a combination of k_0, K_p, and λ.

The formulation presented as equation 3 was the basis of most subsequent analyses of static

jams under steady flow conditions. Beltaos (1983), most notably, substituted expressions for the shear from the water flow and weight of the jam (τ_i and f_3), yielding a direct solution for ice thickness when cohesive stress is negligible:

$$\eta = \frac{BS_o}{2\mu(1-s_i)}\left\{1+\left[1+\frac{(2f_o)^{1/3}\mu(1-s_i)}{s_i}\left(\frac{f_i}{f_o}\right)\frac{\left(\frac{q^2}{gS_o}\right)^{1/3}}{BS_o}\right]^{1/2}\right\} \tag{4}$$

where S_o is the uniform bed slope, q is the unit discharge, and f_i and f_o are the ice and composite Darcy-Weisbach resistance coefficients. Equation 4 has been used to calculate jam thickness and the associated effects on water levels with success, provided good estimates of the coefficients and discharge are available. When using equation 4, one must also keep in mind the underlying assumptions of equilibrium theory: steady, uniform flow; uniform channel section, slope, and jam thickness; and an essentially cohesionless accumulation.

2. Steady Models of Ice Jam Thickness

Most numerical models that address ice jams and their effects on water levels are based on some form of static ice force balance similar to equation 3, coupled with a water flow model. One of the simplest models is a utility program developed by Tuthill et al. (1998) for use with the U.S. Army Corps of Engineers step-backwater program HEC-2. The program, dubbed ICETHK, uses standard output variables from an HEC-2 simulation and calculates ice thickness based on an equation similar to equation 4. Options include width smoothing and ice thickness smoothing, as well as roughness coefficient assignment based on the data of Nezhikhovskiy (1964). The program then automatically updates the HEC-2 input data to reflect the new values of ice thickness and roughness and iterates with HEC-2 until a specified tolerance is met. Since the program considers every reach between successive HEC-2 cross sections as an equilibrium reach, considerable judgment must be used in evaluating the results for the toe and head areas of the jam, where ice thickness does not follow equilibrium theory.

The next level of improvement in ice jam profile models was the inclusion of a variable ice thickness as opposed to the equilibrium value. While these types of models improved on the equation describing the balance of forces on the ice cover, they included only steady water flow. Flato and Gerard (1986) developed the model ICEJAM, which describes the balance of forces on the ice cover over a steady water flow according to

$$\frac{d\eta}{dx} = \frac{s_i \rho g S_w}{2K_p\gamma_e} + \frac{\tau_i}{2\eta K_p\gamma_e} - \frac{k_0 \tan\phi\eta}{B} \tag{5}$$

where S_w is the slope of the water surface, γ_e is the effective unit weight of the cover, and tanϕ is an estimate of λ. Their model calculates the complete ice thickness profile even if there is no equilibrium section. Given input values of discharge, ice properties, roughness, and initial estimates of depth and thickness, the model first calculates water levels by a step-backwater method in the upstream direction and then ice thickness by equation 5 in a downstream direction. Adjustments in thickness at the toe are made according to a prescribed erosion velocity.

Beltaos (1993) describes the RIVJAM model, a steady flow model that includes the seepage flow through the jam in an attempt to better define the thickness near the toe, where grounding may occur. The model solves differential equations for both the water and ice and may proceed in either an upstream or downstream direction. The equation for the ice force balance is similar in form to that of Flato and Gerard (1986) and is given by

$$\frac{d\eta}{dx} = \frac{s_i \rho g S_w}{2K_p \gamma_e} + \frac{\tau_i}{2\eta K_p \gamma_e} - \frac{C_o \eta}{K_p B} \tag{6}$$

where C_o is a shear stress coefficient. Beltaos showed that RIVJAM was able to reproduce measured thickness profiles for a variety of nonequilibrium and potentially grounded jams quite well, with appropriate choices of model parameters, such as the seepage coefficient. Healy and Hicks (1997) compare the ICEJAM and RIVJAM models in detail and provide recommendations for their use.

Daly et al. (1998) describe the modifications to the U.S. Army Corps of Engineers Hydrologic Engineering Center River Analysis System (HEC-RAS) for modeling ice-covered channels. HEC-RAS calculates water surface profiles for steady flow situations and replaces the well-known HEC-2 model. HEC-RAS can accommodate ice-covered channels in two modes: by user-specified ice cover thickness and roughness or by allowing the program to calculate the wide river jam thickness using a force balance equation. The equation representing the force balance is the same as equation 5 when common notation is used. HEC-RAS, similar to the ICEJAM model, solves for the water depth in an upstream direction and ice thickness in a downstream direction. HEC-RAS includes an editor that eases input file generation and has powerful graphics for viewing model results.

The above models are all based on the assumption of steady discharge. While these models have been used with success to replicate the measured water levels associated with past jams, several of the parameters necessary in the models cannot be directly measured. These include the lateral stress coefficient, friction coefficient at the bank, angle of internal resistance, and ice roughness coefficient, as well as the discharge and ice thickness. Several of these unknown parameters (lateral stress, passive pressure, friction at the bank, and porosity) are often lumped together into the coefficient of ice properties, $\mu = k_0 K_p \lambda(1-p)$. While not directly measurable, μ has been back-calculated for many jams and has an accepted range of values between 0.8 to 1.3. Ice thickness profiles have been measured for jams that

have subsequently frozen in place but typically are inferred from shear wall height following jam failure. The true discharge during jam formation is highly suspect. A suitable ice-free gaging station is rarely in the vicinity of a jam location and the local variations of discharge during jamming could be quite large. One is often relegated to using average daily discharge values from an ice-affected gage or the measured discharge beneath a refrozen jam that has stabilized.

The variation in discharge during a breakup jam event and the consequences of using average daily values are illustrated in Figure 1. In this case, the gage was located approximately 1 km downstream from the toe of the jam and remained ice-free during the event. The time of jam formation is evidenced by the drop in discharge at the gage. The time of jam failure is also clearly seen on the figure by the rapid peak and passage of the discharge wave. There is some question as to which discharge to use in modeling the jam: average daily discharge (140 m^3/s), peak discharge at the gage upon jam failure (345 m^3/s), adjusted peak discharge at jam failure (180 m^3/s), or discharge at jam initiation (100 m^3/s). Despite questionable or uncertain estimates of discharge, ice roughness, and jam thickness, measured water levels can be matched quite well by steady flow models with judicious choices of these variables.

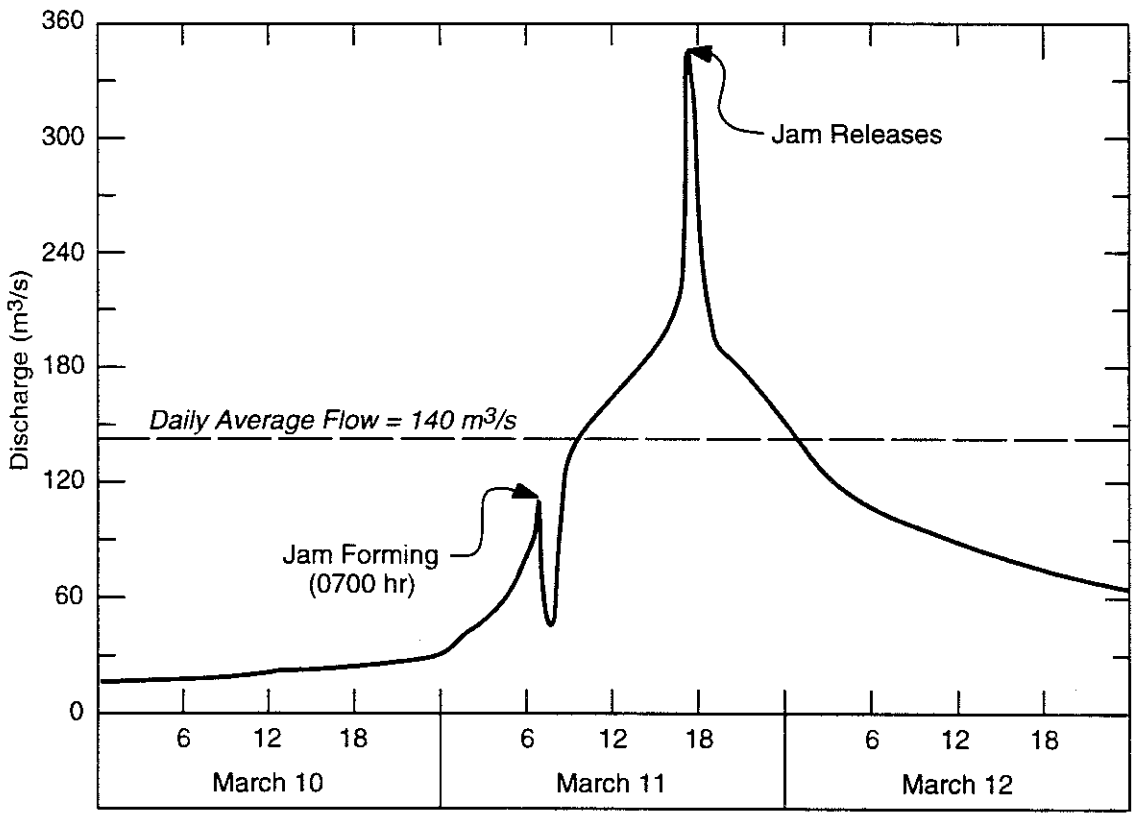

Figure 1. Discharge record during breakup jam initiation and failure.

3. Unsteady Models of Ice Jam Thickness

The problems inherent in selecting the correct discharge to use when modeling ice jamming, as pointed out in Figure 1, leads one to consider the merits of unsteady flow models. Since one of the major forces acting on the ice cover is the shear on the underside from water flow, it follows that correctly representing the discharge with an unsteady flow model should improve the calculation of the ice jam thickness profile. Unsteady flow modeling may be very important for certain breakup jamming events but possibly less important for freezeup events characterized by stable discharges.

One of the simplest extensions to unsteady flow modeling would be adding a static equilibrium thickness cover to an accepted unsteady water model. This is currently being attempted with the U.S. Army Corps of Engineers UNET model. Inclusion of ice routines in the UNET model is still under development; there are two variations at this time. The unsteady water flow equations in UNET have been modified to include the effects of a static, floating cover. A user-specified ice thickness can be included as an input parameter or the program can calculate an equilibrium thickness by an equation similar in form to equation 4. Future modifications will allow calculation of nonequilibrium ice profiles by an equation similar to those used in RIVJAM and ICEJAM.

Breakup jams form and fail in an inherently unsteady way, not only because of discharge but also because of the motion of the ice cover. To better define the processes accompanying jam failure, experiments were conducted in a flume using plastic beads to simulate ice (Zufelt 1992). In those experiments, a multi-layer bead jam was held in place at a reference discharge (Q) by a screen stretched across the flume. The discharge was increased in steps until the bead cover moved. Measurements included water surface slope, cover thickness, and velocity profiles. The properties of the plastic beads were characterized by their porosity and dry angle of repose, which is representative of the angle of internal friction for dry angular materials.

The experiments found two modes of cover failure, which depended on the relative increase in discharge ($\Delta Q/Q$) applied to a stable bead jam. With $\Delta Q/Q$ changes of less than 50%, the cover failed progressively. This type of failure is characterized by movement beginning at the upstream end of the bead jam that slowly progresses downstream through the jam until the entire jam is in motion. Upon reaching the screen, the ice thickens until its strength is sufficient to resist the downstream acting forces. Thickening continues in an upstream direction until the jam is once again stable. With $\Delta Q/Q$ changes greater than 50%, the cover failed completely. This type of failure was much more dynamic, with the entire bead cover seeming to come into motion at once. Thickening begins immediately at the downstream screen and progresses upstream until the entire cover is once again stable.

Figure 2 shows the measured vs. predicted values of jam thickness for several of these jam failure and reformation tests. The measured thickness is the average thickness of the reformed bead jam over its central section (neglecting the toe and head areas). The predicted thickness is that calculated by an equilibrium thickness equation of the form:

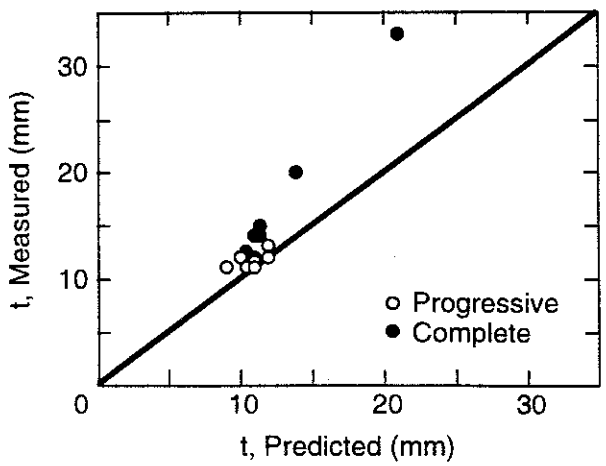

Figure 2. Measured vs. predicted jam thickness following progressive and complete jam failures.

$$\eta = \frac{BS_w}{2\mu(1-s_i)}\left\{1+\left[1+\frac{4R_i\mu(1-s_i)}{s_iBS_w}\right]^{1/2}\right\} \tag{7}$$

where R_i is the hydraulic radius of the ice-affected portion of the flow area, as determined from the measured velocity profiles. The tests that experienced complete jam failures were much more dynamic than the progressive failure tests and show jam thicknesses greater than that predicted by equilibrium theory. This finding points to the importance of unsteadiness in the water discharge, as well as the ice motion, for the complete jam failure situation.

Some jam models have investigated the effects of ice motion on jam profiles. Tsai et al. (1988) developed a jam model to investigate ice transport and jam initiation in rivers. Their model solves the conservation of ice momentum, ice mass, and ice area equations in a Lagrangian form. The values of the ice variables are then used when solving the one-dimensional de Saint Venant equations for unsteady water flow using a four-point finite-difference scheme.

The ultimate in unsteady water and ice modeling is the two-dimensional model developed by Shen et al. (1994) to study the ice transport and jamming in the Upper Niagara River. They formulate the internal ice stress via a viscous–plastic model. A finite-element scheme is used to solve the two-dimensional flow equations, while the ice transport is accomplished by a smoothed particle hydrodynamics method that allows for grounding of ice in the shallow areas. The water and ice motions are coupled through the interaction at the ice/water interface.

Zufelt and Ettema (1997) describe a one-dimensional model, in which the conservation of mass and momentum equations for the water and ice flow are solved simultaneously. That work uses a Preissmann four-point finite-difference scheme to solve the four equations simultaneously for under-ice water depth, water velocity, ice thickness, and ice velocity. The unsteady ice force balance equation (conservation of ice momentum) is given by

$$\frac{\partial \upsilon}{\partial t} + \upsilon\frac{\partial \upsilon}{\partial x} + gs_i\frac{\partial \eta}{\partial x} + g\frac{\partial d}{\partial x} + g(1-s_i)K_p(1-p)\frac{\partial \eta}{\partial x} + \frac{g(1-s_i)}{B}k_0\lambda K_p(1-p)\eta - gS_o - \frac{f_i}{8s_i\eta}(u-\upsilon)^2 = 0 \quad (8)$$

where υ is the ice velocity, d is the under-ice depth, and u is the water velocity. While the model is currently based on channels with a rectangular cross section and assumes that the constitutive relationship for the ice strength can be expressed by the static passive pressure failure theory, it shows the importance of including ice motion in a jam model. The model is used here to demonstrate that ice motion should be included when determining jam thickness and ice-effected water levels.

The study conducted by Zufelt and Ettema (1997) used the simultaneous solution model to examine the effects of bed slope, jam width, jam length, ice strength, and various boundary conditions on the jam thickness profile. Figure 3 shows the inflow hydrograph for a 5-km-long rectangular channel that is 100 m wide and has a bed slope of 0.0005. The initial conditions are a static equilibrium thickness jam with a steady 100-m^3/s discharge. Downstream boundary conditions include zero ice velocity and uniform depth beneath the jam. Upstream boundary conditions include the upstream hydrograph depicted in Figure 3 and an unlimited ice supply, so that ice enters the system at a thickness determined by the uniform version of equation 8, where time-dependent terms are included but space-dependent are terms neglected. The attenuation of the inflow hydrograph is evident in Figure 3 as it travels the 5-km length of the channel. The effects of the ice movement are especially visible at the mid-length of the channel in the form of high-frequency fluctuations in discharge. As ice comes into motion, the resistance on the jam underside is reduced, thereby *locally increasing* the water velocity and discharge. The magnitude of the peak discharge experienced definitely depends on distance for this case of a rapidly increasing and short duration peak (as might be expected downstream from a peaking hydropower plant).

Figure 4 shows the final jam thickness profile for the simultaneous solution test described above. Also shown are jam thickness profiles for a static–unsteady solution and simple equilibrium thickness based on the discharge. For the static–unsteady solution, the unsteady water equations were solved first, followed by a static force balance of the ice similar to that used by RIVJAM or ICEJAM. The equilibrium thickness curve shown is estimated between calculated values of thickness at the upstream end, mid-length, and downstream end of the channel (based on peak discharges in Figure 3). The difference between the equilibrium and static–unsteady profiles illustrates the effects of nonuniformity in depth, water

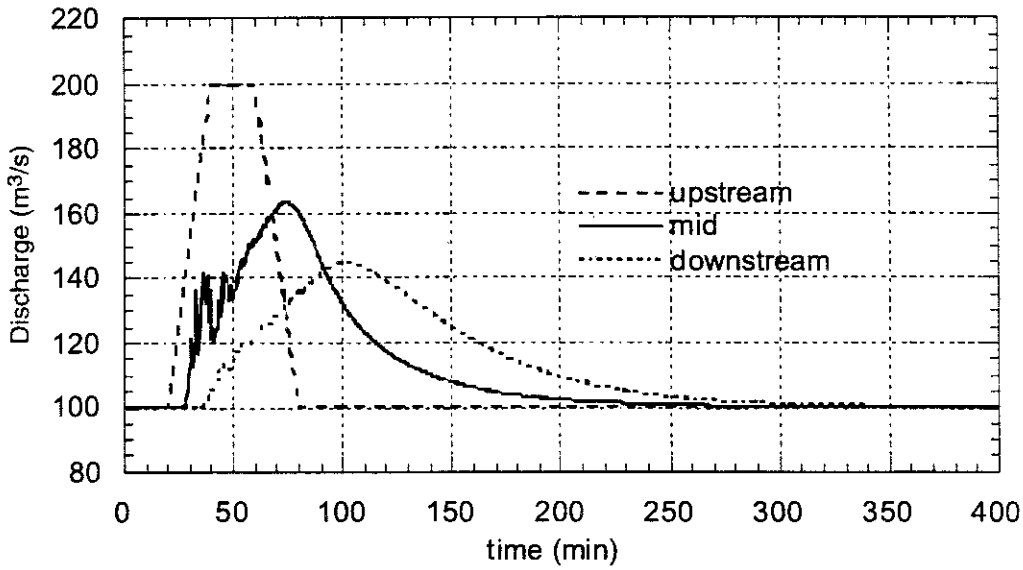

Figure 3. Discharge hydrograph at upstream end, mid-length, and downstream end of 5-km-long channel.

velocity, and jam thickness on the solution. The difference between the static–unsteady and simultaneous solution profiles indicates the effects of ice movement on the solution.

The results in Figure 4 show that equilibrium theory underestimates the jam thickness for this case of a rapidly rising inflow hydrograph, such as might be expected during breakup. Figure 3 also identifies the effects of hydrograph attenuation with increasing channel length. Several other model tests looked at the effect of channel length on the nonuniformity of the

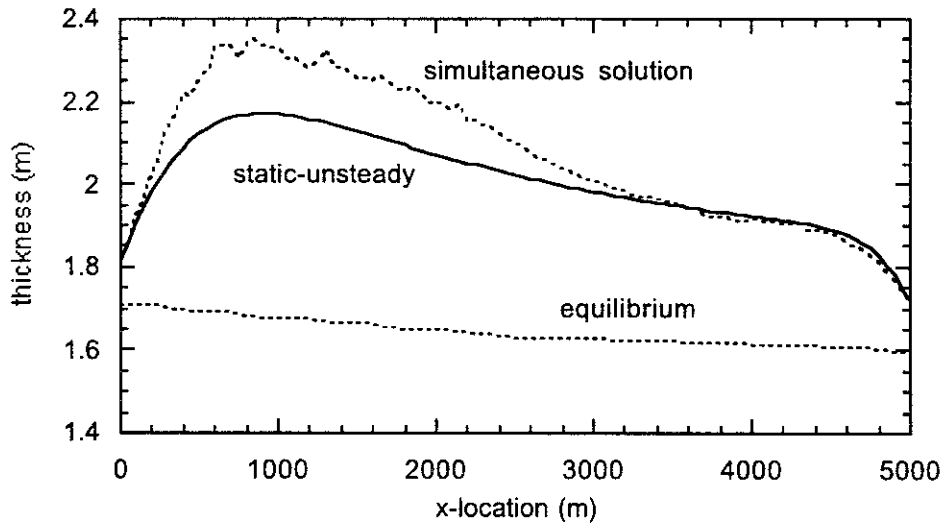

Figure 4. Jam thickness profile using simultaneous solution, static–unsteady model, and equilibrium thickness.

jam thickness profile. Figure 5 shows the final jam thickness profiles for the same inflow hydrograph as in Figure 3 and for channel lengths of 5, 1.0, and 0.5 km. For the shorter channels, the discharge is less attenuated, resulting in more uniform water velocities and hence more uniform jam thicknesses.

4. Dimensionless Stability Parameter

Zufelt and Ettema (in press) also investigated the effects of hydrograph steepness and the duration of the peak flows, as they relate to the wave travel time through a system on the uniformity of the jam thickness profile. Unsteady water flow and ice motion can be very important in determining the jam thickness in cases of rapid flow increases or short duration peaks, as well as in long channels. In addition, however, there are many cases when these effects are relatively minor and equilibrium thickness theory may provide a very good estimate with minimal calculation. A parameter was developed that indicates when the effects of nonuniformity and ice motion should be taken into account and thus when a more complex model for determining jam thickness and water levels should be used.

The dimensionless stability parameter was developed as a measure of the importance of the nonuniform and unsteady ice effects depicted in Figure 4. The parameter was originally termed the dimensionless momentum parameter in Zufelt and Ettema (1997), but since it is based on a form of the equilibrium thickness equation that contains no terms for ice momentum, the name was later changed to avoid confusion. The full conservation of ice momentum in equation 8 is simplified by setting the unsteady and nonuniform terms to zero. For a static ice sheet where $\upsilon = 0$, and rearranging terms,

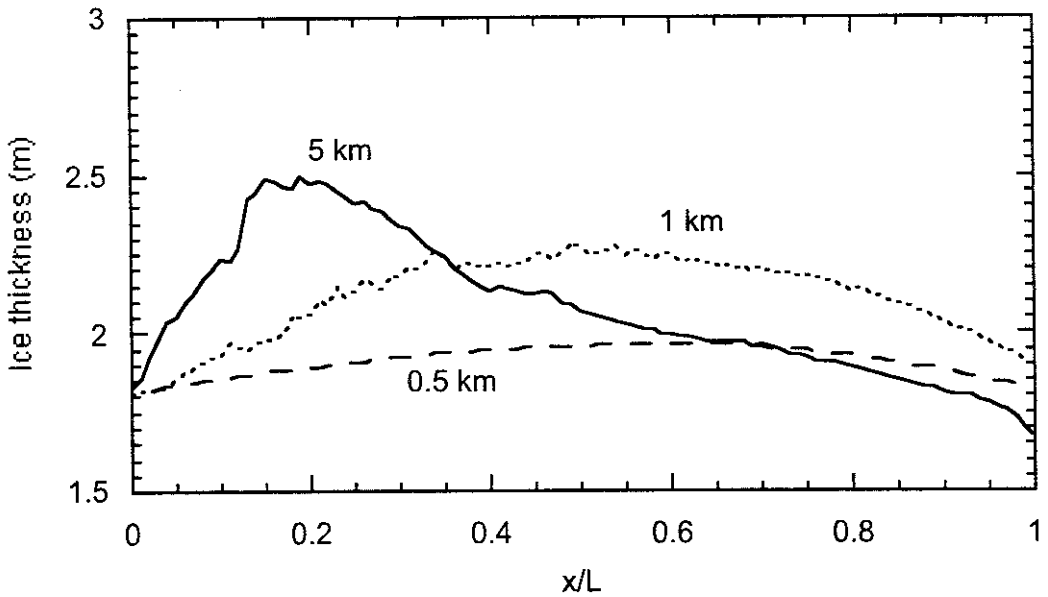

Figure 5. Jam thickness profile for jam lengths of 0.5, 1.0, and 5.0 km.

$$\frac{f_i u^2 B}{8} + gS_o B s_i \eta = g s_i (1-p)(1-s_i) k_0 \lambda K_p \eta^2 \tag{9}$$

which represents the shear on the jam underside and the downstream component of the weight of the jam being balanced by the shear resistance at the banks. If the notation $a + b = c$ is used to describe equation 9, then a/c represents the portion of the jam strength mobilized by the water shear stress. Under the assumption of a wide, rectangular channel, the first term in equation 9 can also be written as

$$a = \frac{f_i u^2 B}{8} = f_i \left(\frac{Q S_o g \sqrt{2B}}{8 f_o} \right)^{2/3} \tag{10}$$

Equation 10 shows that, for a given discharge, the a term has a constant value. Equation 9 is then balanced by adjusting the value of jam thickness to the equilibrium value, giving a value of a/c at the limit of stability. Suppose, for example, that previous events had left the thickness at a greater level than the equilibrium value associated with the present discharge. This could happen if the discharge receded following a shoving and thickening event. This would result in equation 9 no longer being in balance and would represent a condition of greater jam stability. The a/c ratio would be decreased because the discharge had been reduced since the time that equation 9 was in balance. For a subsequent rise in discharge, the jam should remain stable for a longer period before failure, thus resulting in lower ice velocities and a decreased effect of ice momentum on the final jam thickness once failure takes place. Also, for a given initial jam thickness (whether at the limit of stability or not), a smaller discharge rise has less effect on jam thickness than does a larger one. Finally, a larger relative discharge increase was shown to have more of an effect than a smaller one in the experiments outlined in Zufelt (1992). For instance, unsteadiness and ice momentum would be expected to influence the final jam thickness more for an increase from 100 to 200 m^3/s than for an increase from 200 to 300 m^3/s.

These trends are expressed in the dimensionless parameter, which includes initial jam conditions that indicate how close the jam is to the limit of stability, as well as the relative increase in discharge expected. The parameter is

$$\Omega = \left(\frac{a}{c} \right) \left(\frac{\Delta Q}{Q_{in}} \right) = \frac{f_i u^2 B}{8 g s_i (1-p)(1-s_i) k_0 \lambda K_p \eta^2} \left(\frac{\Delta Q}{Q_{in}} \right) \tag{11}$$

where Q_{in} is the initial water discharge and ΔQ is the expected change in discharge. The resulting dimensionless parameter is the product of the initial state of stability of the jam and the relative discharge increase applied to cause an instability.

Many tests were made with the simultaneous solution model at a variety of bed slopes, ice

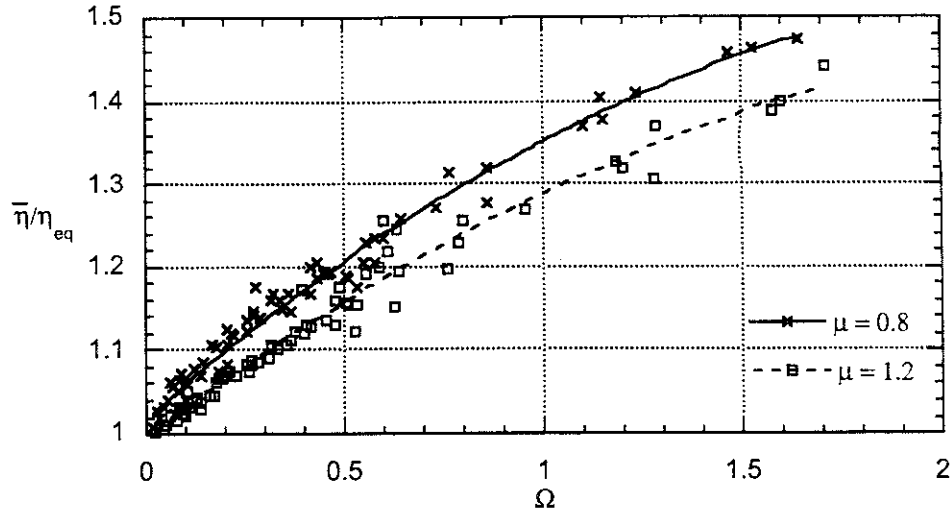

Figure 6. Dimensionless jam thickness vs. stability number.

strengths, initial discharge, and discharge increases. For all tests, the rate of discharge increase was the same as depicted in Figure 3. The final jam thickness profile for each test was compared to the equilibrium thickness (calculated by equation 4) for the peak inflow discharge for that run. The values of Ω were plotted against the length-averaged thickness normalized by the calculated equilibrium thickness. Figure 6 shows the plots for ice strength coefficient values of 0.8 and 1.2. The smaller values of Ω represent smaller relative increases in discharge or greater initial stability of the jam (smaller *a/c* values), or both. The jam thicknesses calculated by the more complex unsteady model at smaller Ω values are not very much different from jam thicknesses calculated by simple equilibrium theory. In cases where the relative change in discharge is small or the jam is not close to the limits of stability, the equilibrium thickness calculation provides a very good estimate of jam thickness with only minor violations of the underlying assumptions attendant to equilibrium theory.

As an example of the use of Figure 6, consider a freezeup jam that has formed below a hydropower plant over the weekend during the off-peak discharge cycle. Given a bed slope of 0.0005, $f_i = 0.12$, $f_o = 0.10$, off-peak $Q = 75$ m^3/s, peaking $Q = 150$ m^3/s, $\mu = 0.8$, and $B = 100$ m, one can calculate that the equilibrium ice thickness is 1.33 m and the value of $\Omega = 0.409$. From Figure 6, this means that the average jam thickness below the dam following peaking would be approximately 1.18 times the calculated equilibrium thickness and most likely will have a highly unsteady profile, such as that exhibited in Figure 4. On the other hand, if the scenario is for a jam that formed in a relatively uniform reach at a discharge of 75 m^3/s, which has since receded to 60 m^3/s and is expected to increase over the next two days to 85 m^3/s, one would expect less of an effect, owing to unsteadiness and ice motion. For the same river and ice characteristics, the value of $\Omega = 0.141$ and the expected increase over equilibrium jam thickness would only be on the order of 5–6%.

Zufelt and Ettema (in prep) discuss the effects of the rate of rise of the hydrograph and the duration of the sustained peak flow on the curves such as those shown in Figure 6. In general terms, faster rise times shift the curves upward (a greater degree of unsteadiness). Duration of peak flow is related to the length of the river system by the water disturbance travel time (open water wave speed). If the duration of the peak flow is greater than the travel time for the reach length of interest, the peak flow will have enough time to establish itself throughout the entire system. If the duration of the peak flow is less than the travel time, significant discharge attenuation can occur, similar to that depicted in Figure 3.

5. Conclusions

There are many models available for the calculation of ice jam thickness and its effect on water levels. The models range from the very simple equilibrium thickness theory equation for jam thickness to more complex models that include unsteady water and ice motion. Equilibrium theory has many inherent simplifying assumptions that should be considered for its use. Minor violations of these assumptions may only result in minor errors in calculated thickness. Highly unsteady discharge, however, induces nonuniform variations in water depth, water velocity, and ice motion that may result in very nonuniform jam thickness profiles. Equilibrium theory may well under-predict the thickness of these profiles.

A dimensionless jam stability parameter is introduced that provides a measure of initial jam stability and relative degree of unsteadiness from an expected discharge increase. The results of the simultaneous solution model of Zufelt and Ettema (1997) are used to develop a figure that displays the variation of average jam thickness from equilibrium theory with increasing nonuniform and unsteady effects. Steeper hydrograph increases result in greater nonuniformity of the jam thickness profile. Longer hydrograph peak duration or shorter initial jam length reduces the nonuniformity of the thickness profile.

References

Beltaos, S. 1983. River ice jams: theory, case studies and applications. *ASCE Journal of Hydraulic Engineering*, Vol. 109(10), 1338–1359.

Beltaos, S. 1993. Numerical computation of river ice jams. *Canadian Journal of Civil Engineering*, Vol. 20(1), 88–99.

Daly, S.F., Brunner, G., Piper, S., Jensen, M., and Tuthill, A.M. 1998. Modeling Ice-Covered Rivers using HEC-RAS. *Proceedings, 9th International Conference on Cold Regions Engineering, Duluth, MN*, pp. 373–383.

Flato, G.M., and Gerard, R. 1986. Calculation of ice jam profiles. *Proceedings, 4th Workshop on Hydraulics of River Ice, Montreal, Quebec, Canada*, Paper C-3.

Healy, D., and Hicks, F.E. 1997. A Comparison of the RIVJAM and ICEJAM Ice Jam Profile Models. Water Resources Engineering Report WRE 97-H1, Department of

Civil and Environmental Engineering, University of Alberta, Edmonton, Alberta, Canada.

Kennedy, R.J. 1958. Forces involved in pulpwood holding grounds - I. Transverse holding grounds with piers. *The Engineering Journal, Engineering Institute of Canada*, Vol. 41, 58–68.

Nezhikhovskiy, R.A. 1964. Coefficients of roughness of bottom surface on slush-ice cover. *Soviet Hydrology: Selected Papers*, American Geophysical Union, No. 2, pp. 127–150.

Pariset, E., and Hausser, R. 1961. Formation and evolution of ice covers on rivers. *Transactions of the Engineering Institute of Canada*, Vol. 5(1), 41–49.

Pariset, E., Hausser, R., and Gagnon, A. 1966. Formation of ice covers and ice jams in rivers. *ASCE Journal of Hydraulic Engineering*, Vol. 92(HY6), 1–24.

Shen, H.T., Su, J., Lu, S., and Wake, I. 1994. A two-dimensional model for dynamic ice transport and jamming in the Upper Niagara River. *Proceedings, IAHR Ice Symposium 1994, Trondheim, Norway*, Vol. 2., pp. 724–733.

Tsai, S.M., Shen, H.T., and Shen, H.H. 1988. Dynamic transport of river ice and jam initiation. Report No. 88-2, Dept. of Civil and Environmental Engineering, Clarkson University, Potsdam, NY.

Tuthill, A.M., Wuebben, J.L., and Gagnon, J.J. 1998. ICETHK User's Manual: Version 1. U.S. Army Cold Regions Research and Engineering Laboratory, Special Report 98-11.

Zufelt, J.E. 1992. Modes of ice cover failure during shoving and thickening. *Proceedings, IAHR Ice Symposium 1992, Banff, Alberta, Canada*, Vol. 3, pp. 1507–1514.

Zufelt, J.E., and Ettema, R. 1997. Unsteady Ice Jam Processes. U.S. Army Cold Regions Research and Engineering Laboratory, CRREL Report 97-7.

Zufelt, J.E. and Ettema, R. (in press). A Fully Coupled Model of Ice Jam Dynamics." Submitted to *ASCE Journal of Cold Regions Engineering*.